MORPHOLOGY OF QSO HOST GALAXIES — A LOOK AT THE SED

A.H. ANDREI[1,2,3,4], B. COELHO[3], S. ANTÓN[5,6]
[1] Observatório Nacional/MCTI
Rua Gal. José Cristino 77, Rio de Janeiro, RJ CEP 20921-400, Brasil
e-mail: oat1@ov.ufrj.br
[2] SYRTE/Observatoire de Paris
Avenue de l'Observatoire 61, Paris 75014, France
[3] Observatório do Valongo/UFRJ
Ladeira do Pedro Antônio 43, Rio de Janeiro, RJ CEP 20080-090, Brasil
[4] Osservatorio Astrofisico di Torino/INAF
Strada Osservatorio 20, Pino Torinese, TO 10025, Italia
[5] Instituto de Astrofísica de Andalucía/CSIC
Glorieta de la Astronomia s/n, 18008, Granda, España
[6] Faculdade de Ciências/Universidade de Lisboa
Tapada da Ajuda 1349-018, Lisboa, Portugal

ABSTRACT. The Gaia Initial QSO Catalogue presents several characteristics of its 1,248,372 listed objects, among which the optical morphological type. From this a program studies the host galaxies of QSOs present in the SDSS up to its 8th release, based on retrieving a data bank of images in the five *ugriz* colors for the 105,783 objects spectroscopically found as QSOs. The first scope of this program is to study QSOs for which the isophotes of the host galaxy are not pronounced, so that the centroid determination is not affected for those fundamental grid-points of the Gaia Celestial Reference Frame. Since the target images come from relatively short exposures, we developed an approach to access disturbances of the target PSF relatively to the nearby stars. Here we focus on the first results for absolute magnitude of QSOs combining the SDSS colors and the SED library from Gaia.

1. INTRODUCTION

The latest, updated, and fully corrected version of the Gaia Initial QSO Catalog (GIQC, Andrei et al., 2014), produced by the CU3 GWP-S-335-13000 contains 1,248,372 objects, of which 191,372 are considered and marked as Defining ones, because of their observational history and existence of spectroscopic redshift. Also objects with strong, calibrator-like radio emission are included in this category. The Defining objects represent a clean sample of quasars. The remaining objects aim to bring completeness to the GIQC at the time of its compilation. For the whole GIQC the average density is 30.3 sources per sq.deg., practically all sources have an indication of magnitude and of morphological indexes, and 90% of the sources have an indication of redshift and of variability indexes (Fig. 1). QSOs are crucial targets to define the Gaia Celestial Reference Frame (GCRF), and accordingly on board means are capable of classifying them. The QSO classification contains three major orientations: getting a zero-contaminants QSO sample to determine the GCRF; deriving the most complete QSO sample based on the full Gaia data; and determining astrophysical parameters for each QSO. The determination itself of a Gaia source as a QSO is planned to rely primarily on comparison of the photometric output against a template of spectral energy distributions (SED), and secondarily on astrometric observables, variability analysis and a reliable initial list of known QSOs.

It is now largely accepted that depending on whether the jets from where the radio emission emanates are seen head-on or face-on the disagreement between the radio and optical centroids can reach several milliarcseconds. Since the GCRF will define the Celestial Reference Frame to sub-μas level and the number of sources tying it to the current ICRF is of less than 100, these outliers must be flagged off the soonest. And the situation can be still more adverse, noticing that most of Gaia quasars are at redshift smaller than 1 and that those belonging to the current ICRF are much closer yet. Coherently with the findings of the Gaia WP Initial QSO Catalog, in the Gaia data treatment all QSOs will be handled as

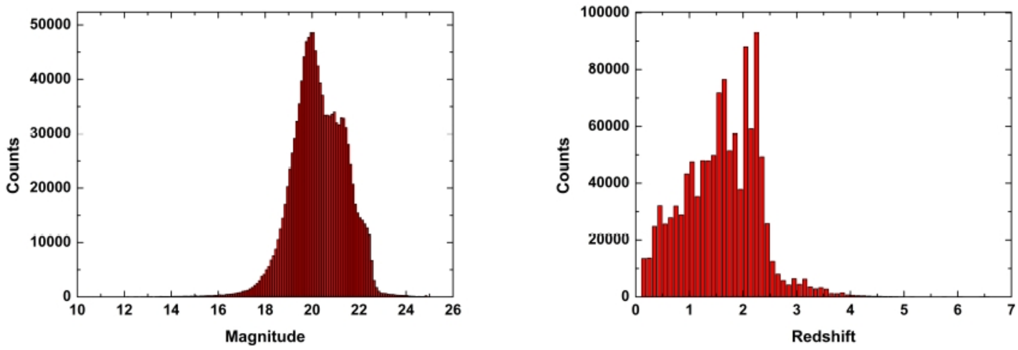

Figure 1: Magnitude and redshift counts of the GIQC sources.

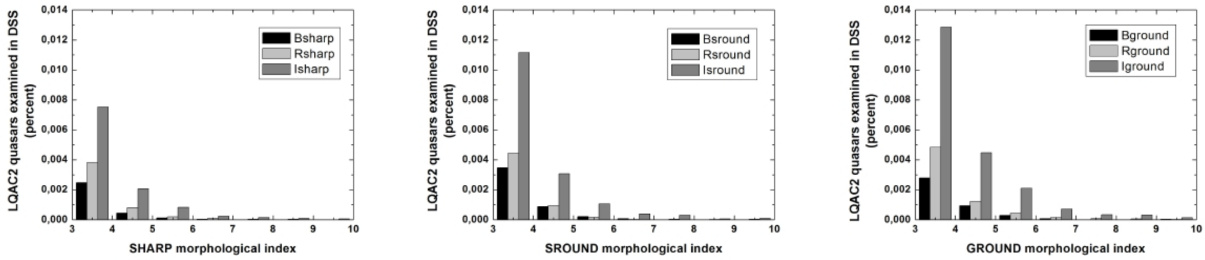

Figure 2: Binned distribution of the morphological indexes, for quasars that are markedly non-pointlike. Data from the LQAC2 catalogue (Souchay et al., 2012) and B, R, I plates from the DSS (The Digitized Sky Survey was produced at the Space Telescope Science Institute under U.S. Government grant NAG W-2166).

extended sources in order to model for the host galaxy isophotes. Yet, there is a loss of astrometric precision in both extremes, when the host galaxy is very bright and extensive, and when the source is not pointlike but there aren't enough photons to properly fit the structure underneath (Fig. 2). Thus in the GIQC the morphological classification derives from comparing the target PSF characteristics against the local PSF characteristics, as given by the average from nearby stars of similar magnitude (Andrei et al., 2010).

The absolute magnitude of quasars is used in the GIQC as starting point to calculate the variability indexes and to interpret the morphological indexes. From the absolute magnitude the luminosity and mass are worked out, and hence the radius of the accretion disk is calculated (Morgan et al., 2010; Shen et al., 2008). From these the probability of accretion disk or torus instabilities to induce optical variability are derived (Popovic et al., 2012). It is also from the absolute magnitude of the quasar that features of the host galaxy can be estimated (Serjeant et al., 2009), from which the morphological indexes are understood.

2. THE DETERMINATION OF QSOs' ABSOLUTE MAGNITUDE

The determination of the absolute magnitude is fundamental to discuss the QSOs and host galaxies properties from the astrophysical and cosmological points of view. Usually in the literature the absolute magnitude of QSOs is simplified by a power law continuum. A complete description, allowing for the blue-bump and the presence of emission lines will give a more reliable measure of the light coming from the AGN, thus improving a separate discussion of the central engine and extended environment, and a better characterization of the QSO itself.

We develop a program to study the host galaxies of QSOs present in the SDSS up to its 8th release. The main observational data thus comprises a large retrieved data bank of images in the five *ugriz* colors for the 105,783 objects spectroscopically found as QSOs, within frames large enough to contain tens of comparison stars and several field galaxies. From it the *ugriz* magnitudes are combined with the Gaia

Quasar Synthetic Spectra library (QSSL, Claeskens et al., 2006) to derive the absolute magnitudes.

Initially we de-convolve the apparent magnitudes from the bandpass and integrated efficiency of the *ugriz* filters (Fukugita et al., 1996) to re-construct the incoming flux density.

Next the absorption and reddening are taken into account. For the galactic absorption the Schlegel et al. (1998) high resolution ($\sim$ few arc-minute) 100μ intensity map is used from the equatorial coordinates. The tables return the V band extinction as function (B-V), which can be extended to other bands and passbands. After that the Lyman-α forest absorption must be accounted for. The models are controversial, because the size and density of hydrogen clouds and blobs vary in redshift. We adopted the model of Meiksin (2006) that computes the attenuation for different system of astronomy filters, including the SDSS *ugriz*.

Intergalactic dust includes from micro particles to large molecules. There are models and examples of increasing dust column density along the line of site. However, for most cases the amount of reddening is uncorrelated to the amount of extinction due to the Lyman-α forest. And the lines associated to gas accompanying the dust are better explained at the rest frame. This is adopted the model of Hopkins et al. (2004). This model assumes the reddening toward quasars as dominated by SMC-like dust at the quasar redshift. It computes the color attenuation based of a large sample of SDSS QSOs. Following this model we calculated the modal values – or mean value where the samples are too small – that correspond to the intrinsic colors of QSOs at a given redshift; the excess to it must be corrected to the obtained rest-frame color (hence absolute magnitude).

Finally, at the rest frame, we combine the redshift from the SDSS with knowledge of the Spectral Energy Distribution (SED) to derive the absolute magnitudes in different bands and passbands. The QSSL coverage is complemented by the SWIRE template library (Polletta et al., 2006). Their extent are as bellow.

- QSSL: wavelength – λ from 2,500.5Å to 10,499.5Å, step 0.5Å; spectral index – α from -4 to $+3$, step 1; flux – W (arbitrary units) from 10^2 to 10^6, step $\times$ 1.58489; redshift – z from 0.0 to 5.5, step 0.1019.
- SWIRE: wavelength – λ from 1,000.5Å to 1,000 μ, step $20\times\log(\lambda)$ Å; spectral index – α for QSO type 1 (face on) and QSO type 2 (edge on); flux – W (arbitrary units) from 1 to 20; redshift – z on the rest frame.

3. RESULTS

The obtained absolute magnitudes follow well what is expected from the current astrophysical models (Fig. 3). Both the effects of the blue-bump and of the cosmological increase of brightness are well recovered. Also the variation of the spectral indexes is in agreement with the unified model (Fig. 4).

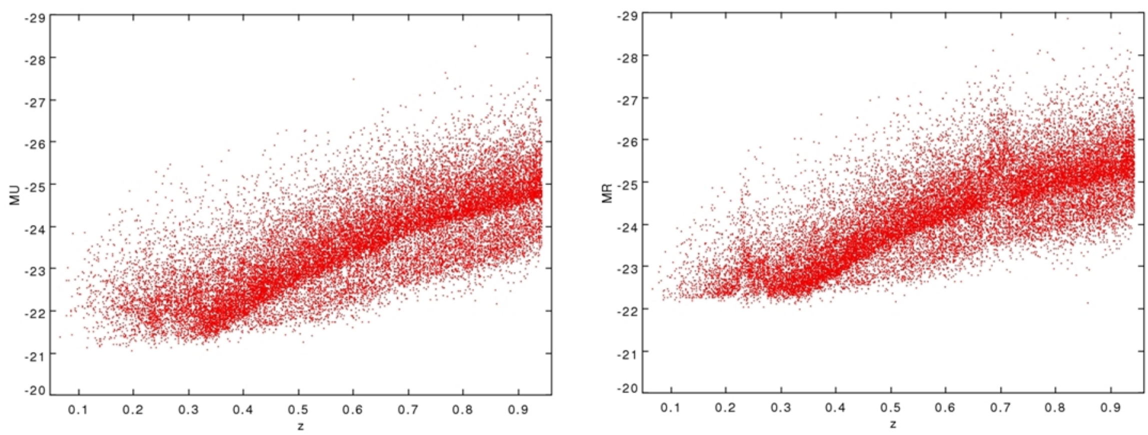

Figure 3: Calculated absolute magnitudes. The cosmological increase towards a maximum around z=2 is clear. The absolute magnitudes are generally brighter than those in the literature because the SED and emission lines are included.

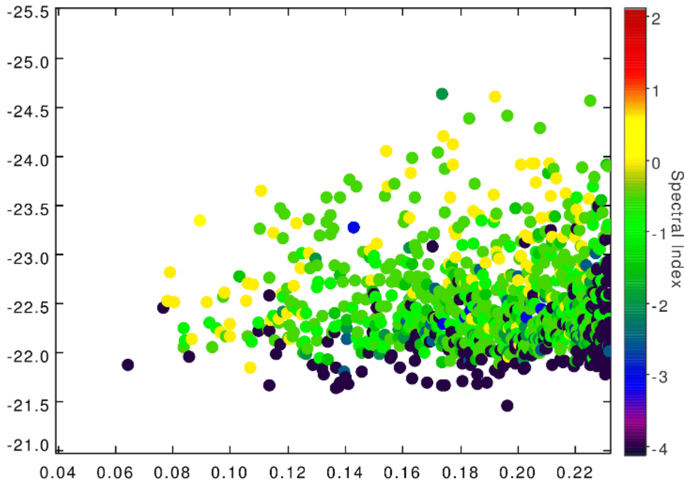

Figure 4: Spectral index distribution resulting from the fitting of the best SED for the calculation of the absolute magnitudes.

These results are being continued to discuss the morphological output in Gaia observations along different LSFs (line spread function), in special for the ICRF quasars that will contribute to the radio-to-optical link of the GCRF, in which the reconciliation of the centroids is of paramount importance.

Acknowledgements. A.H.A. thanks the CNPq/BR Bolsa de Pesquisa and the CAPES/BR AEX grant. Funding for the SDSS has been provided by the Alfred P. Sloan Foundation, the Participating Institutions, the N.S.F. and the U.S. Dept. of Energy Office of Science.

4. REFERENCES

Andrei, A.H., et al., 2010, "Gaia Initial QSO Catalogue for Gaia — The MDB version", Gaia Research Note GAIA-C3-SP-GPA-AA-002-1.

Andrei, A.H., et al., 2014, "The Gaia Initial Quasar Catalog", In: Proc. Journées 2013 "Systèmes de Référence Spatio-Temporels", N. Capitaine (ed.), Observatoire de Paris, pp. 84–87.

Souchay, J., et al., 2012, "The Second Release of the Large Quasar Astrometric Catalog", A&A, 537, 99.

Claeskens, J.-F., et al., 2006, "Identification and Redshift Determination of Quasi-stellar Objects with Medium-band Photometry: Application to Gaia", MNRAS 367, 879.

Fukugita, M., et al., 1996, "The Sloan Digital Sky Survey Photometric System", AJ, 111, 174.

Hopkins, P.F., 2004, "Dust Reddening in Sloan Digital Sky Survey Quasars", AJ, 128, 1112.

Meiksin, A., 2006, "Colour Corrections for High-redshift Objects Due to Intergallactic Attenuation", MNRAS, 365, 833.

Morgan, C.W., et al., 2010, "The Quasar Accretion Disk Size-black Hole Mass Relation", ApJ, 712, 1129.

Polletta, M. del Carmen, 2006, "Chandra and Spitzer unveil Heavily Obscured Quasars in the Chandra/SWIRE Survey", ApJ, 642, 673.

Popovic, L.C., et al., 2012, "Photocentric Variability of Quasars caused by Variations in their Inner Structure: Consequences for Gaia Measurements", A&A, 538, 107.

Schlegel, D.J., et al., 1998, "Maps of Dust Infrared Emission for Use in Estimation of Reddening and Cosmic Microwave Backgrouns Radiation Foregrounds", ApJ, 500, 525.

Serjeant, S., et al., 2009, "The Evolution of Star Formation in Quasar Host Galaxies", MNRAS, 397, 265.

Shen, Y., et al., 2008, "Biases in Virial Black Hole Masses: An SDSS Perspective", ApJ, 680, 169.